

INSTALLATION OF DRIVEN PILES IN LIMESTONE AREAS

**S.L.Lee¹, Y.K.Chow², K.Y.Yong², G.P.Karunaratne³,
and K.Y.Wong⁴**

SYNOPSIS

A method is described to estimate the load carrying capacity of individual driven piles bearing in limestone. The method uses a recently developed wave equation model for the analysis and enables the estimation of the end bearing afforded by the limestone, including piles with weak end bearing or damaged toe. While the method accounts for cavities in the underlying limestone formation affecting the capacity of individual piles, it cannot predict the capacity of a group of closely-spaced piles which is more seriously affected by the presence of cavities. The application of this method is demonstrated by a case study of precast reinforced concrete piles driven through soft cohesive soil to bearing in limestone.

INTRODUCTION

The major problem arising from piles driven into limestone is the prediction of the end bearing afforded by the limestone. Core samples of limestone, under unconfined compression tests, generally show large variation in compressive strength between samples, with the strength being dependent on the number of fissures and cavities present in the sample. As a result, the estimation of the end bearing afforded by the limestone using static capacity estimation methods can be unreliable. This problem is compounded by the driving action during pile installation which can result in extensive fragmentation of the limestone.

A possible method to estimate the load carrying capacity of a pile driven into limestone is by the method of set matching using a wave equation analysis. In this method, the load carrying capacity of a driven pile is estimated using a bearing

-
1. Professor, Dept of Civil Engng, National University of Singapore, 10 Kent Ridge Crescent, Singapore 0511
 2. Senior Lecturer, Dept of Civil Engng, National University of Singapore, 10 Kent Ridge Crescent, Singapore 0511
 3. Associate Professor, Dept of Civil Engng, National University of Singapore, 10 Kent Ridge Crescent, Singapore 0511
 4. Executive Engineer, L & M Geotechnic Pte Ltd, Singapore

curve of soil resistance versus pile set, generated from soil parameters that are determined from a correlation of the load test capacity and set of a reference test pile. In the analyses presented in this paper, a recently developed one-dimensional wave equation model presented by Lee *et al.* (1988) was used. This new model uses conventional soil mechanics parameters which can be determined in the laboratory or correlated to conventional soil properties. A major improvement of this model over that presented by Smith (1960) is the proper modelling of energy losses through the propagation of shear waves through the surrounding soil mass. This mode of energy dissipation from the pile-soil interface is commonly known as geometric or radiation damping.

METHOD OF ANALYSIS

The method of estimating the load carrying capacity of a driven pile by set matching was first proposed by Smith (1960) and demonstrated by Forehand & Reese (1964). Subsequently, this method of load carrying capacity estimation received acceptance particularly in the United States and Canada. For Example, the Canadian Foundation Engineering Manual (1985) recommends its usage. However, in using this method, its limitations must be realised. Strictly, the method is applicable for piles driven into soils which do not exhibit thixotropic effects. Under this condition, a correlation of a pile load test and field set in the wave equation analysis can be used to estimate the soil parameters at the site. The input energy assumed in the analysis must be representative of the hammer performance. The effects of input energy on the predicted capacity was discussed by Tavenas & Audibert (1977). Once these soil parameters have been established, bearing curves can be generated. Although this method of set matching is strictly applicable for non-thixotropic soils, practical solutions can also be generated for thixotropic soils, provided one recognises that these thixotropic effects are somewhat accounted for in the soil parameters determined by the correlation in the wave equation analysis. The bearing curves are only applicable for estimating the load carrying capacity of driven piles with similar elapsed time after driving as the reference pile. An alternative method that can take into account the soil set-up using the model presented by Lee *et al.* (1988) was described by Chow *et al.* (1988). This method determines the soil resistance immediately after driving and uses the reference pile load test capacity to determine the soil's regain in strength or set-up, up to the time load testing for the reference test pile. However, Chow *et al.* (1988) showed that both methods (direct correlation of load capacity method and soil set-up method), when properly used, can result in the satisfactory estimation of the load carrying capacity of piles for a similar elapsed time after driving as the reference test pile.

Wave equation analysis using the new model shows that the pile set determined from a single blow analysis may not be representative of the set determined from a multiple blow analysis that takes into account the soil residual stresses resulting from preceding hammer blows. This is particularly true for a pile driven into soil which has a large tip resistance. Driving stresses, in particular tensile stresses, are increased by the action of residual stresses. Therefore, multiple blow analysis should be carried out for determining driving stresses and pile set for piles driven into limestone.

The procedure described herein provides a direct correlation of load carrying capacity of pile and pile set. From the soil investigation report, an estimate is made of the unit shaft friction applicable for the piles at the site. The toe resistance for a reference test pile is estimated using the load carrying capacity determined from the load test. A wave equation analysis is then carried out with the load carrying capacity determined from the load test as the soil resistance during driving. The wave equation analysis is used to determine the soil shear modulus, G_s , of the limestone by set matching. Note that the soil shear modulus represents the biggest uncertainty in the input parameters required in this new model. If the pile is driven through cohesive soil, the shear modulus of the cohesive soil at the shaft may be estimated using the correlation with the undrained shear strength of the soil. A G_s/c_u ratio of 150, commonly assumed in the analysis of axially loaded piles, may be used. For cohesionless soil, a G_s/σ'_v ratio of 200 may be used, where σ'_v is the effective vertical stress. This ratio of G_s/σ'_v for the cohesionless soil was determined from back-analysis of driving records and load tests (Chow *et al.*, 1988 and Wong *et al.*, 1987). The predicted set by the wave equation analysis will not match the field set initially. By changing the soil shear modulus for the limestone, set matching can be achieved after a few trials. The soil shear modulus determined for the limestone is then used to establish a ratio of shear modulus to unit base resistance, G_s/q_b .

The determined G_s/q_b ratio, unit skin friction, hammer efficiency and cushion/capblock properties can then be used to generate bearing curves for various penetration depths. These curves are generated by varying the toe resistance afforded by the limestone. The shear modulus of the limestone is varied with each variation in toe resistance, using the G_s/q_b ratio determined from the correlation. This manner of analysis results in a family of curves (for various penetration depths) that will allow the toe resistance of a pile to be estimated by set matching. The method described is summarised in a flowchart in Fig. 1.

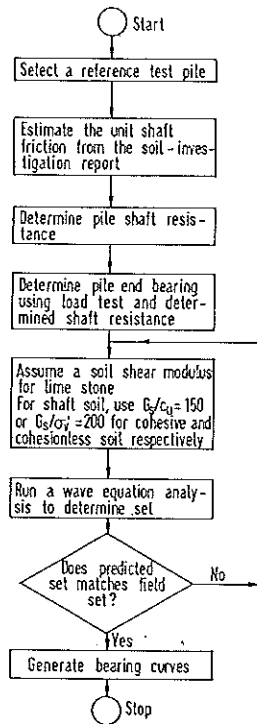


Fig. 1 Flowchart for the determination of the G_s/q_b ratio of the limestone for the reference test pile

Since more than one test pile is usually available for a site, the load carrying capacity of the other test piles can be estimated and compared with the field results. These comparisons can further enhance confidence in using the determined bearing curves if the estimated load carrying capacities agree reasonably well with the field results. These comparisons are useful since the first reference test pile may be damaged in the installation process. If the pile is broken for example, the length and end bearing resistance used in the wave equation analysis will result in a poor estimate of the G_s/q_b ratio for the limestone. If the estimated and field capacities do not agree reasonably well with the majority of the test piles, an alternative test pile may be required to re-estimate the soil shear modulus of the limestone.

INSTALLATION IN LIMESTONE AREAS

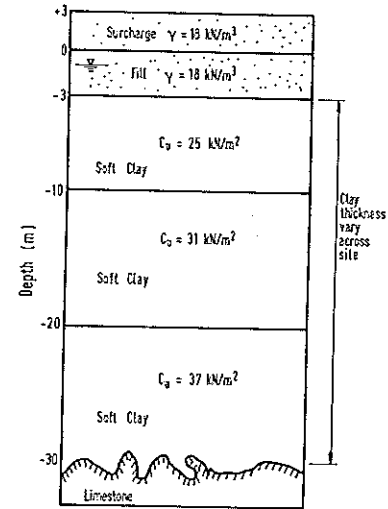


Fig. 2 Generalised soil profile at site

CASE STUDY

The following case study illustrates the use of the method described in the preceding section to estimate the load carrying capacity of the piles driven into limestone with the possibility of toe damage or weak end bearing. Estimates of the load carrying capacity of these piles are essential to evaluate the overall structural stability of the super-structure if these piles are not compensated by driving additional piles.

Site and Soil Conditions

The site under study is proposed for the development of five-storey low cost flats (no basement). This site is located in a former tin mining area in Kuala Lumpur, Malaysia. The area under consideration consists of two ponds which have been infilled and has been treated with a combination of 3 m of surcharge and vertical band drains.

The subsoil conditions are typical of ex-mining land. The soils overlying the limestone and granite bedrock consist of alluvial deposits, which are the original

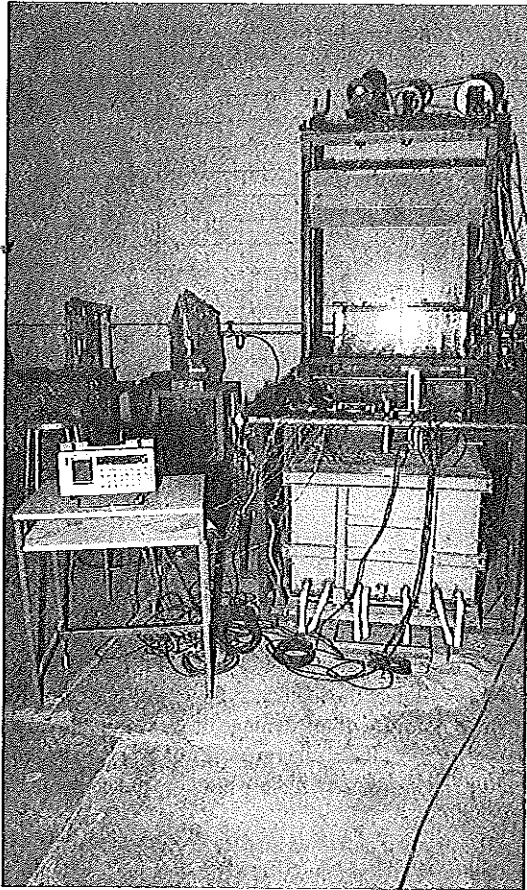


Plate 1. View of the Complete Test Setup

overburden, and/or tailing soils. The alluvial deposits often occur in the form of medium stiff to stiff clay and medium dense to dense sand while the tailing soils are usually loose sand and very soft silty clay.

The estimated soil shear strength at various depths is shown in Fig. 2. The depth to limestone is expected to vary from 10 m to 30 m. Unconfined

INSTALLATION IN LIMESTONE AREAS

compression tests on the limestone samples indicated large variation in strength, typically between 15 MPa to 60 MPa.

Pile type and driving hammers

Three sizes of reinforced concrete piles were proposed for this site. These piles consist of Hume-Balken RC piles (Grade 45) with Oslo point at the pile tip. The sizes of the piles and their proposed working loads are shown in Table 1. These working loads are based on 25 percent of the concrete cube strength.

The estimated average pile penetration based on soil investigation at the site is expected to be 20 m. Piles driven for two blocks of flats indicated that over 50 percent of the piles are less than 18 m and 80 percent of the piles are less than 27 m.

Three hammer sizes were used at the site : a one tonne drop hammer, and Kobe 13 and Hera 800 diesel hammers. The ram of these diesel hammers were 1.3 tonnes and 0.8 tonnes respectively. The diesel hammers were favoured over the drop hammer in the driving of the piles due to their speed of installation.

Test Piles

Seven piles (TP1 to TP7) were load tested by the maintained load test method and the constant rate of penetration method. The pile data and load test results for the maintained load test are summarised in Table 2. Stress wave measurements were also carried out for these test piles and a number of other piles. Unfortunately, a minor calibration problem in the instruments recording these stress waves rendered the estimation of the load carrying capacity of these piles from the stress waves measurements unreliable. However, these measurements are still useful for indicating the structural integrity of the piles and allow some 'visualisation' of the soil distribution along the piles. Since the stress wave measurements were not properly calibrated, they were not used in the analysis presented herein.

Wave Equation Analysis

A reference test pile, TP1, was selected for the purpose of determining the G_s/q_b ratio for the limestone by the wave equation analysis. The pile was driven by a one tonne drop hammer in the final stage of the installation. The pile

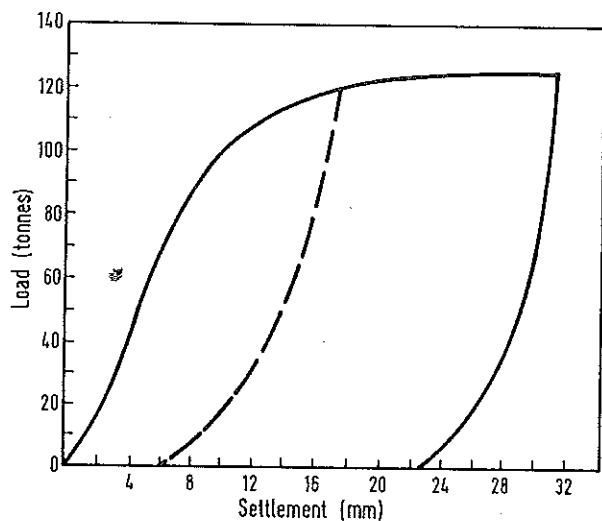


Fig. 3 Load-settlement curve for pile TP2

capacity, pile set and driving stresses were estimated assuming the efficiency of the drop hammer to be 0.7. A wooden capblock and cushion were used. The capblock and cushion were made up of several pieces of plywood. The unit skin friction of the soft clay mobilised during driving was estimated to be 15 KPa. This value is reasonable for the soil strength at the site (Fig.2). The wave equation analysis for the reference test pile, TP1, indicated that the G_s/q_b ratio for the limestone was 140. This ratio was compared with that determined using the load-settlement curve (maintained load), shown in Fig. 3, for pile TP2. The shaft resistance of TP2 was neglected in the analysis and the pile is treated as a free standing column. Since the pile is only 10 m in length, the neglect of the shaft resistance is not expected to affect the determined soil shear modulus of the limestone significantly. The tip settlement of the pile is determined from the difference between the measured top settlement and the elastic compression of the pile. The soil shear modulus of the limestone is then determined from the static soil stiffness coefficient of a rigid punch on the surface of an elastic half-space. The G_s/q_b ratio determined for TP2 was about 120 which agree reasonably well with that using TP1 from the wave equation analysis.

The estimated load carrying capacity and the maximum driving stresses for

Table 2 Summary of wave equation analysis

Ref.	File Size (mm)	Pile Length (m)	Hammer	Mass (tonnes)	Drop (m)	hammer Efficiency	Set per 10 blows (mm)	Predicted Capacity (tonnes)	ML Test Capacity (tonnes)	Max. Compression Stress (MPa)	Max. Tensile Stress (MPa)	Remarks
TP1*	235 x235	38.8	Drop	1.0	1.22	0.7	23	82	83	23	6.5	*Reference test pile to estimate Soil properties
TP2	235 x235	10.4	Drop	1.0	1.22	0.7	8	119	120	25	6.0	
TP3	175 x175	24.4	Drop	1.0	1.10	0.7	11	81	70+	35	3.0	
TP4	200 x200	30.5	Drop	1.0	1.35	0.7	8	95	90+	32	4.0	
TP5	235 x235	31.1	K13	1.3	2.30	0.4	7	120**	120+	27	5.5	**No stress-waves measurements for this pile. Backfigured hammer efficiency to give measured capacity
TP6	175 x175	19.5	H800	0.8	2.5	0.3	11	80	70	29	2.2	Back-figured hammer efficiency to give measured capacity.
TP7	175 x175	18.5	H800	0.8	2.5	0.3	5	72	70+	31	3.6	

Note *Twice working load

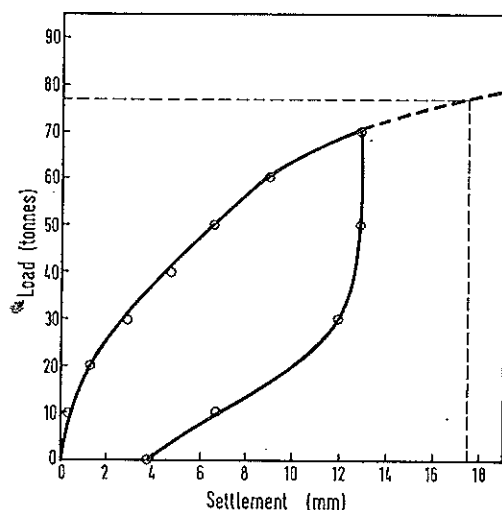


Fig. 4 Load-settlement curve for pile TP3

the other test piles driven with the one tonne drop hammer (TP2, TP3 and TP4) are also shown in Table 2. Note that for piles TP3 and TP4 the estimated capacities were higher than that for the maintained load tests at twice the working load. Fig. 4 shows the load-settlement curve for pile TP3. By extrapolating the load-settlement curve, the load carrying capacity at settlement corresponding to 10 percent of the pile width (17.5 mm) for TP3 was 77 tonnes, compared to the predicted value of 81 tonnes. For TP4, the load carrying capacity at settlement corresponding to 10 percent of the pile width (20 mm) was about 100 tonnes compared to 95 tonnes predicted. Therefore in general, good agreement between estimated and load tested capacities were achieved. One other possible reason, in addition to the satisfactory estimation of the G_s/q_b ratio of the limestone, for the good estimations of the load carrying capacity of test piles TP2, TP3 and TP4 is that all the piles were tested after the same elapse time (6 days) after driving. Any possible thixotropic effects are likely to be similar for these piles and is accounted for in the G_s/q_b ratio determined from the analysis of the reference test pile, TP1.

For test piles TP5, and TP6 and TP7, driven with diesel hammers Kobe 13 and Hera 800 respectively, the use of a hammer efficiency of 0.7 was inappro-

priate. The use of this efficiency resulted in predicted driving stresses that far exceeds the compressive strength of the concrete. The efficiency of the Kobe 13 was determined to be 0.4 from back-analysis of TP5 and that of the Hera 800 was 0.3 using TP6. The G_s/q_b ratio used was that determined by TP1. Using the hammer efficiency of 0.3 for the Hera 800 hammer, the estimated bearing capacity for TP7 resulted in good agreement with the load tested capacity (Table 2). It is interesting to note that although the stress wave measurements have a slight calibration problem, these measurements also indicated low efficiencies for the diesel hammers. The average efficiency indicated by the stress wave measurements was about 0.35 for the diesel hammers at various stages of driving.

Bearing Curves For Toe Resistance Estimation

Bearing curves for three penetration depths were generated for the diesel hammers, Kobe 13 and Hera 800 for the 200 x 200 mm pile and 175 x 175 mm pile respectively, using the hammer efficiencies determined. These curves are shown in Figs. 5 and 6 for the 175 x 175 mm pile and for the 200 x 200 mm pile respectively. The penetration depths of 10 m, 20 m and 30 m were expected to cover the variation in the limestone profile as indicated by piles driven for the two blocks of flats mentioned earlier. These curves were truncated at twice the proposed working load of the piles since the required factor of safety was 2. From these curves, the toe resistance can be estimated by subtracting the skin friction from the estimated load carrying capacity.

DISCUSSIONS

The amount of energy delivered by a diesel hammer depends mainly on the soil resistance encountered during driving. In the generation of bearing curves, it is commonly assumed that the energy delivered by the diesel hammer is constant. Although this assumption is not strictly true, there is no alternative choice in generating bearing curves that are suitable for general use for a site. It would be impractical to run a wave equation analysis to match the set using the observed hammer drop for each pile.

It is interesting to note that the soil resistance for a particular set is dependent on the pile penetration as shown in Figs. 5 and 6. This is rational and in accordance with the theory of wave propagation. The longer pile loses more energy to the soil mass through increased radiation damping and hysteresis due to soil

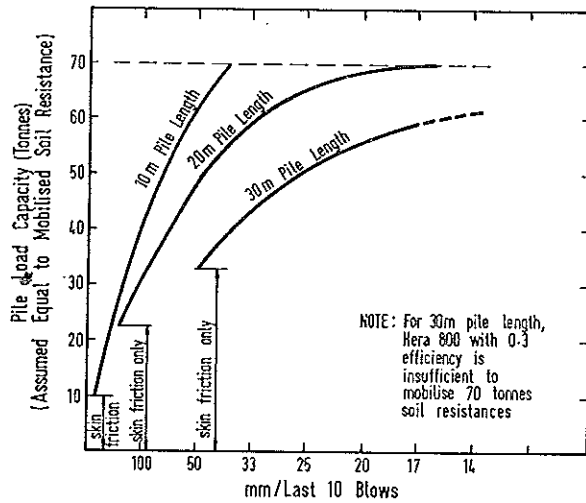


Fig. 5 Bearing curves for 175 x 175 mm piles driven by the Hera 800 hammer at 0.3 efficiency

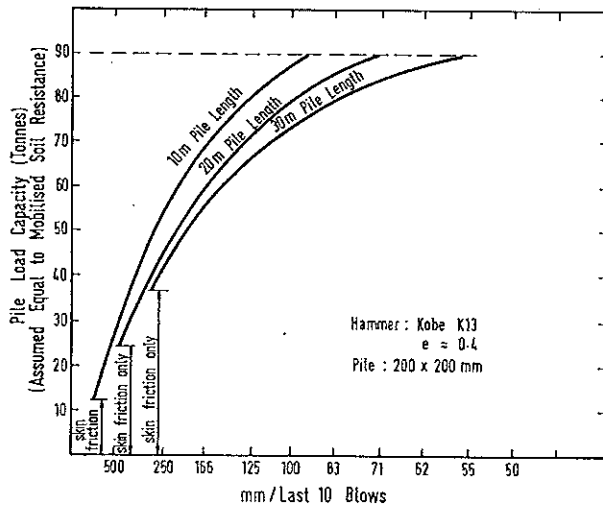


Fig. 6 Bearing curves for 200 x 200 mm piles driven by the Kobe 13 hammer at 0.4 efficiency

plasticity. Since the input energy is constant, less energy is now available in the longer pile to overcome the tip resistance, resulting in lower set. Note that in Fig. 5, the input energy of the Hera 800 (0.3 efficiency) is insufficient to mobilise 70 tonnes of soil resistance for the 30 m penetration.

When the pile set is small (for example 10 mm/10 blows), the load carrying capacity of a pile estimated from the bearing curve may only represent a lower bound. Hence, the proper interpretation of a bearing curve is important. If interpreted indiscriminately, it would appear that a 30 m pile has a smaller load carrying capacity than a 10 or 20 m pile. Strictly, these curves represent the soil resistance that can be mobilised by the driving system. As the resistance increases through deeper penetration, the pile may approach refusal under the assumed driving system. The conclusion, that the estimated load carrying capacity of a pile with small set being a lower bound, is also reflected in the stress wave matching method. When the pile set is small, changing the toe resistance to a larger value in the wave equation analysis, after stress wave matching is achieved, results in little change in the predicted stress wave profile. However, under easy driving (large sets), the soil resistance is fully mobilised and it is

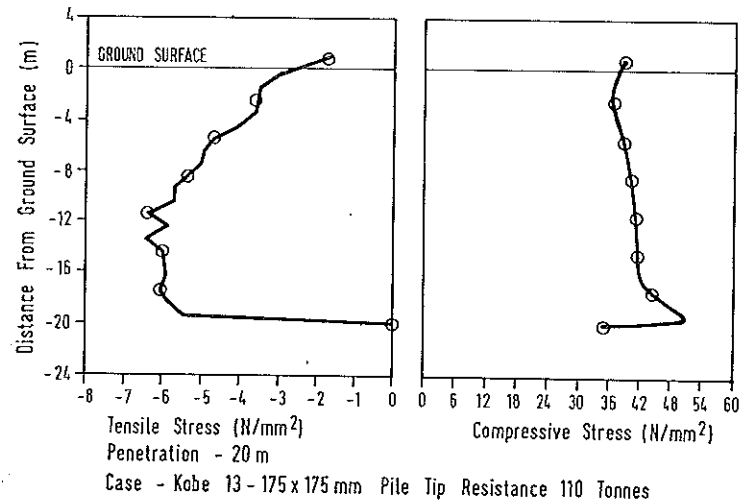


Fig. 7 Maximum driving stresses distribution in the 175 x 175 mm pile driven by the Kobe 13 at 0.4 efficiency

therefore reasonable to relate the soil resistance during driving to the load carrying capacity of the pile. In this case, changing the toe resistance in the stress wave matching method will be reflected by a change in the predicted stress wave profile. Therefore, the bearing curves in Figs. 5 and 6 may be used to estimate the load carrying capacity of piles with weak toe resistance, since, large sets are generally expected for these piles.

The predicted peak compressive and tensile driving stresses for the 175 x 175 mm pile driven by the Hera 800 at 0.3 efficiency to a set of about 10 mm/10 blows were 31 MPa and 3.0 MPa respectively while those for the 200 x 200 mm pile driven by the kobe 13 at 0.4 efficiency were 33 MPa and 5.0 MPa respectively.

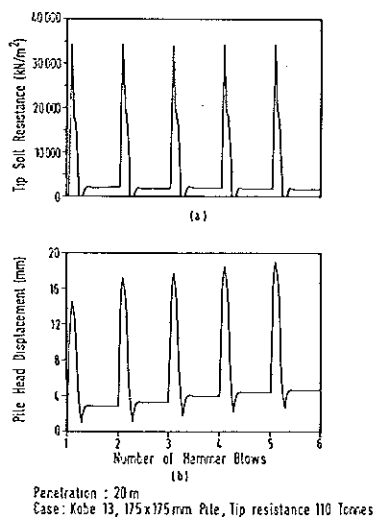


Fig. 8 Pile top displacement and tip soil stress responses for the 175 x 175 mm pile driven by the Kobe 13 at 0.4 efficiency

An additional simulation was carried out to evaluate the suitability of the Kobe 13 to drive the 175 x 175 mm pile, in particular to investigate if driving stresses will be excessive. In this simulation, a large tip resistance (110 tonnes) was used to simulate the condition when the pile encounters competent limestone. The predicted driving stresses are shown in Fig. 7. It is evident from Fig.

7 that the peak compressive stress of about 52 MPa exceeded the concrete cube strength. The effect of the large tip resistance reinforces the oncoming compressive stress wave resulting in the high compressive stresses at around the tip. Therefore, although there may be no evidence of failure at pile top due to compressive waves, toe crushing may occur. Whereas the higher compressive stress due to the large tip resistance is expected, the predicted large peak tensile stress of 6.5 MPa is not. To visualise why this peak tensile stress may be generated, Fig. 8 (a) shows the pile tip stress response for five consecutive hammer blows (multiple blow analysis). These blows were applied when the tip velocity due to the preceding blow vanishes. Note that there are instances when the tip is stress free during pile tip rebound resulting in a boundary condition where tensile waves can develop. Fig. 8 (b) shows the displacement response near the pile top. Note that the first hammer blow overestimated the pile set. For the soil resistance used in the simulation, the set determined from the second to fifth blow shows an average set of about 4 mm/10 blows which is practically refusal. The predicted temporary compression of the pile is about 14 mm. The results of this simulation indicated that the Kobe 13 is unsuitable for driving the 175 x 175 mm pile.

CONCLUSIONS

A method for estimating the load carrying capacity of individual driven piles bearing in limestone is presented. This method uses a recently developed wave equation model (Lee *et al.*, 1988) for the analysis. The method was demonstrated by a case study where load test results of seven piles were available. Using the method presented, bearing curves were generated which enable the estimation of the load carrying capacity of individual piles, including piles with possible toe damage. It should be noted that while the method accounts for cavities in the underlying limestone formation affecting the capacity of individual piles, it would not provide information on pile group capacity affected by these cavities. This latter subject is, however, beyond the scope of the present paper.

REFERENCES

- ANON (1985), *Canadian Foundation Engineering Manual* Canadian Geotechnical Society.
- CHOW, Y.K., KARUNARATNE, G.P., WONG, K.Y., & LEE, S.L. (1988), "Prediction of load-carrying capacity of driven piles", *Canadian Geotechnical Journal* 25 (1), 13-23.

- FOREHAND, P.W. & REESE, J.L. (1964). "Prediction of pile capacity by the wave equation", *Journal of Soil Mechanics and Foundation Division*, ASCE, 90(20), 1-25.
- GIBSON, G.C. & COYLE, H.M. (1968), "Soil damping constants related to common soil properties in sand and clay", *Report no. 125-1, TTI, Texas, A & University*.
- LEE, S.L., CHOW, Y.K., KARUNARATNE, G.P. & WONG, K.Y. (1988), "Rational wave equation model for pile-driving analysis", *Journal of Geotechnical Engineering*, ASCE, 114(3), 306-325.
- TAVENAS, F.A. & AUDIBERT, J.M.E. (1977), "Application of the wave equation analysis to friction piles in sand", *Canadian Geotechnical Journal*, 14(1), 43-51.
- SMITH, E.A.L. (1960), "Pile driving analysis by the wave equation", *Journal of Soil Mechanics and Foundation Division*, ASCE, 86(4), 35-61.
- WONG, K.Y., CHOW, Y.K., KARUNARATNE, G.P. & LEE, S.L. (1987), "Driveability of piles and the effects of followers", *Geotechnical Engineering*, 18(2), 167-184.

APPENDIX I – NOTATIONS

The following symbols are used in this paper,

c_u – undrained shear strength,

q_b – unit base resistance of limestone

f'_{cu} – concrete cube strength,

G_s – shear modulus of limestone/soil,

σ'_v – effective vertical stress

γ – unit weight of soil